Available online at www.sciencedirect.com

ScienceDirect

journal homepage: www.elsevier.com/locate/bbe

Original Research Article

A novel exoskeleton robotic system for hand rehabilitation – Conceptualization to prototyping

Jamshed Iqbal [a,b,*], Hamza Khan [a], Nikos G. Tsagarakis [a], Darwin G. Caldwell [a]

[a] Advanced Robotics Department, Istituto Italiano di Tecnologia (IIT), Genova, Italy
[b] Department of Electrical Engineering, COMSATS, Islamabad, Pakistan

ARTICLE INFO

Article history:
Received 27 April 2013
Received in revised form
4 January 2014
Accepted 10 January 2014
Available online 5 February 2014

Keywords:
Hand rehabilitation
Motion assistance
Robotic exoskeleton
Wearable robotics

ABSTRACT

This research presents a novel hand exoskeleton rehabilitation device to facilitate tendon therapy exercises. The exoskeleton is designed to assist fingers flexion and extension motions in a natural manner. The proposed multi-Degree Of Freedom (DOF) system consists of a direct-driven, optimized and underactuated serial linkage mechanism having capability to exert extremely high force levels perpendicularly on the finger phalanges. Kinematic and dynamic models of the proposed device have been derived. The device design is based on the results of multi-objective optimization algorithm and series of experiments conducted to study capabilities of the human hand. To permit a user-friendly interaction with the device, the control is based on minimum jerk trajectory generation. Using this control system, the transient response and steady state behavior of the proposed device are analyzed after designing and fabricating a two-fingered prototype. The pilot study shows that the proposed rehabilitation system is capable of flexing and extending the fingers with accurate trajectories.

1. Introduction

Hands offer autonomy in a human life by offering physical interaction and grasping capabilities. Motivated by the central role of hands in our daily life, researchers have been targeting its imitation using robotic systems. Thanks to technological advancements in mechatronics, such robotic systems greatly improve both the sensing and manipulation strengths of a human. It has been predicted that by 2024, people will use fashionable and portable exoskeleton based robotic systems for interaction in social life [1].

Hands are the most vulnerable limbs having high chances of suffering from disabilities like injuries or strokes especially in elder persons. The most commonly influenced neurological domain of stroke is the motor system [2]. The disabled motor deficit usually is the impaired hand function [3]. Results of a study [4] carried out to evaluate the needs of stroke patients showed that the most desired function in recovery of an impaired hand is its ability to regain strength to perform Activities of Daily Living (ADL). Rehabilitation therapy during post-stroke activities can significantly facilitate the recovery process. Physiotherapists usually conduct these therapy exercises manually or occasionally use simple devices offering passive assistance. Results of therapeutic treatment indicate that the chances of impaired hand recovery are low [5]. Studies report that weakness in both finger flexor and extensor muscles is one of the factors for hand impairment [6].

* Corresponding author at: Department of Electrical Engineering, COMSATS, Islamabad, Pakistan.
E-mail address: iqbal.jam@gmail.com (J. Iqbal).

0208-5216/$ – see front matter
http://dx.doi.org/10.1016/j.bbe.2014.01.003

Repetitive active training schemes based on activities requiring finger flexion and extension motion could restore the grasping and object manipulation capabilities of an impaired hand [7]. There is an increasing belief that novel therapy procedures using active exoskeleton based exercisers or assistive devices can be potentially helpful in reducing the recovery times and the treatment cost.

The primitive functions of a hand exoskeleton are to monitor the human hand/fingers motions and to apply forces at the fingers. Such devices are aimed at emulating the grasping constraints by transmitting the kinesthetic feedback at finger level. Studies have shown that rehabilitative training of hand using mechatronic systems has enhanced the outcomes of rehabilitation [8]. Robot-based rehabilitation offers precise execution of therapy procedures and enhances exercises repeatability. Autonomous robots can share the workload of therapists conducting the rehabilitation paradigms. Moreover, integration of robotics with Virtual Reality (VR) and acquisition of quantitative data can facilitate hand rehabilitation by optimization of therapy procedures and analysis of patients' response.

This paper is organized as follows: Section 2 presents details of the existing hand rehabilitation devices based on exoskeletons. It also highlights the novelty of the proposed rehabilitation system. The concept and model of the system is presented in Section 3. Section 4 introduces the design requirements and optimization of the device while Section 5 deals with its control part. The fabricated prototype and results are reported in Section 6. Finally Section 7 comments on conclusion.

2. Literature review and novelty of the proposed system

The complex structure and intricateness of human hands offer high dexterity and precise manipulation capability. These, however, impose great difficulties on the development of a hand exoskeleton system. Multi-Degree Of Freedom (DOF) in our hands with small moving parts and availability of limited space for mechatronic placement make the development task further challenging. Compared to exoskeleton systems for lower extremity and arm rehabilitation, the devices for hand or fingers are few, but are receiving growing attention. The reported devices for the hand vary widely in terms of Range Of Motion (ROM), no. of actuated DOFs, design strategy and nature of intended movements.

Therapy procedures for rehabilitation can be based either on passive or active movements. Passive devices offer limited rehabilitation features and have the capability to support few DOFs. No sensory feedback data is available to therapists. Many of these devices apply a simple continuous motion and cannot exert forces perpendicular to the finger digits. Jace H440 [9] is a commercially available Continuous Passive Machine (CPM) that operates in two modes: warm-up mode and dynamic tension mode. On-board microprocessor senses the resistance of the tissues and adjusts ROM automatically. Researchers of Harbin Institute of Technology (HIT) developed a passive rehabilitation device that provides bidirectional force feedback with 4 DOF/finger [10]. The proposed CPM is actuated by two motors and provides both position and force feedbacks to therapist. Another passive rehabilitation device, HandSOME (Hand Spring Operated Movement Enhancer) [11] is aimed at coordination of natural grasping motion. The device, consisting of four bar linkage mechanism, compensates for flexor hypertonia by extension of the finger joints.

A rehabilitation device essentially demands capability of bidirectional assistance i.e. finger flexion as well as its extension. Primarily, due to this reason, most of the hand exoskeleton systems used in VR applications e.g. [12–17] do not find significant potential in rehabilitation.

Due to the restricted space at the hand, most of the hand exoskeleton systems with only few exceptions [18,19], are remotely actuated. The torque/force is transmitted to the exoskeleton mechanism through Bowden cables or tendons. Researchers of Salford University have proposed a four finger novel hand exoskeleton based exerciser [20] with 7 active DOF. The actuators are placed on ground and tendons having low friction transmit the bidirectional forces. The major milestone during the device design was to offer dexterity with adequate ROM. Introducing interactive VR in rehabilitation, the device has been integrated within a hand therapy system to permit a physiotherapist to conduct hand exercises and to analyze motion data. Wege et al. developed another tendon driven hand rehabilitation system having 4 DOF/finger [21]. Actuated with a single DC motor, the device can exert bidirectional forces on the finger phalanges based on torque control. Link lengths have been designed to allow nearly full ROM. HANDEXOS proposed by the researchers at SSSA, Italy has been aimed at simplifying complexity of the exoskeleton in terms of its actuation, mechanism and structure while ensuring full hand mobility [22]. Each finger incorporates one passive and three active rotational joints while the only translational joint is passive. The active joints provide flexion and extension of finger joints while abduction and adduction is permitted by passive rotational joint. With an under-actuated mechanism and tendon transmission, an index finger prototype has been realized. Other examples of systems using cable as transmission media include HEXORR (Hand EXOskeleton Rehabilitation Robot) [23] and Beihang University device [24]. Cable based systems suffer from inherent friction and associated issues when compared with their direct-driven counterparts.

A rehabilitation device should offer free palm so that patients can have natural interaction with the objects. Few reported devices e.g. Rutgers Hand Master II [18] is a pneumatically actuated device having pistons in the inner side of the palm. The device provides force feedback and has been used for stroke rehabilitation [25]. In addition to palm, a rehabilitation device should also let each fingertip of a patient's hand free for exploiting tactile cues. HandCARE [26] is a Cable-Actuated REhabilitation device which uses cable loops fixed at the end of each finger. Promising attribute of the device is a clutch system that can actuate all the five fingers with a single actuator. Amadeo by Tyromotion Inc. [27] is a commercial rehabilitation device that offers fingertips control of each hand digit. The system offers a therapist to select among three modes: active, completely passive or assistive. Rehabilitation devices exerting forces on the distal finger phalanges of the hand provide limited control over proximal and middle joints. This can be a source of inaccurate joint kinematics in abnormal patients.

Most of the above mentioned systems do not consider the design optimization by taking into consideration the requirements of the natural hand. The work in [28] presented an optimized design of a hand exoskeleton haptic interface based on the isotropy in the robot's workspace. However, the device has not been used for rehabilitation. The optimization procedure should also consider the fact that a rehabilitation exerciser preferably has the capability to exert forces perpendicular to the finger phalanges to avoid pulling or pushing in a wrong direction. The works in [13,21,29] present some design requirements of a hand exoskeleton system but only subjective description has been mentioned. We believe that the design and development of a hand exoskeleton system should be based on concrete numerical data, which can, in some degree, corresponds to the human hand strength and capabilities.

Portability in a rehabilitation device can broaden its potential applications. A portable device may be used for prosthetics as well as for assistance to perform ADL. However, most of the reported hand exoskeleton rehabilitation devices, with very few exceptions [9–11,30] lack portability.

Table 1 presents the comparative review of popular systems intended for hand rehabilitation. Both the passive and active systems have been sub-categorized based on force/torque transmission mechanism i.e. cable-driven or linkage based. The in-depth review of the existing systems has pointed out that there is no device presented to-date that encompasses all the distinguishing features listed below in a single system.

- Direct-driven
- Bi-directional forces of up to 45 N
- Optimized link structure
- DOF/Finger
- Low complexity
- Portability
- Back-drivability
- Palm free
- Provision of position as well as force feedback

3. Robot kinematic and dynamic models

The proposed hand exoskeleton is an under-actuated Revolute–Revolute–Revolute (RRR) mechanism comprising of three serial planar links and is fixed to the wearer at a single point. Such a manipulator like configuration, composed of rigid links interconnected by joints can be designed to function like a human arm/hand [31]. The attachment point can be located either at the proximal or the middle segment of the finger [32]. Under-actuated mechanism reduces the requirements on the number of actuators and also permits passive adaptation of each finger according to the shape of grasped object. The complete system resides on the dorsal side of the hand, thus preserving patient's palmar area and fingertips free for interaction with objects encountered in daily life. The exoskeleton robot is powered with a single actuation unit which resides at the base of the first robotic joint. The conceptual design of one finger of the proposed rehabilitation system is presented in Fig. 1a. The preliminary requirement of bidirectional motion (flexion and extension) for the proposed rehabilitation device lead to define the desired finger trajectory (Fig. 1b) to be used in the robot modeling.

3.1. *Kinematic model*

The forward kinematic model of the proposed exoskeleton determines the position and orientation of the robot's end-effector based on its joint angles [33]. To derive the kinematic model, the links of the robot have been described using well-known Denavit–Hartenberg (DH) parameters (Table 2).

Based on these parameters, the corresponding transformation matrices for each link of the robotic arm have been written

Table 1 – Review of hand rehabilitation systems.

	Force transmission	System	Developer	DOF	Actuators	O/p force, Torque	Remarks
CPM	Linkage	HandSOME	Brokaw et al.	1	Passive	4 N m	Apply extension torques to cope flexor hypertonia
		WaveFlex	Otto Bock	1	DC motor	42 N (reversing)	Full composite fist flexion
	Cable	HIT Machine	Fu et al.	4	DC motor	1 N m	Exerts forces ⊥ to finger phalanges
Active Exo. Systems	Linkage	HWARD	Takahashi et al.	3	Pneumatic	15 N	Assistive
		Rutgers Master II	Bouzit et al.	4	Pneumatic	16.4 N	Direct-drive actuators are located in palm
		Hand Robot Alpha-II	MIT	1	Brushless DC motor	120 N	Fingers move together
		HEXORR	Schabowsky et al.	2	Brushless DC motor	0.13 N m	CPM/Active Exo.
		IntelliArm	Ren et al.	1	DC motor	2.5 N m	Single DOF for hand.
	Cable	CyberGrasp	Immersion Inc.	5	DC motor	12 N	Used with CyberGlove
		Salford Univ. Exo.	Sarakglou et al.	7	DC motor	20 N	VR based exerciser
		TU Berlin Exo.	Wege et al.	4	DC motor	?	Actuators reside on-ground
		HANDEXOS	Chiri et al.	5	DC motor	?	Underactuated mechanism
		HandCARE	Dovat et al.	?	DC motor	15 N	VR training

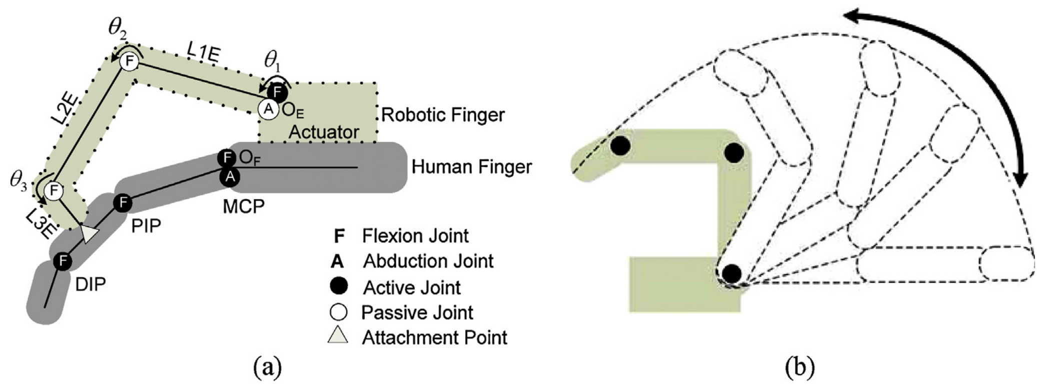

Fig. 1 – (a) Conceptual design of the proposed exoskeleton finger and (b) finger flexion cycle showing the desired trajectory.

Table 2 – DH parameters of the proposed hand exoskeleton.

Symbol	Joint (i)			
	1	2	3	4
α_{i-1}	0	0	0	0
a_{i-1}	0	L_{1E}	L_{2E}	L_{3E}
d_i	0	0	0	0
θ_i	θ_1	θ_2	θ_3	0

using the general form of the transformation matrix for each link (expressing joint 'i' in its previous neighboring joint 'i − 1'). Exploiting the compound transformation property, these individual matrices when multiplied yielded the overall transformation from the end-effector to the base of the robot (see Appendix A).

$$ {}^{0}_{4}T = \begin{bmatrix} C_{123} & -S_{123} & 0 & L_{1E}C_1 + L_{2E}C_{12} + L_{3E}C_{123} \\ S_{123} & C_{123} & 0 & L_{1E}S_1 + L_{2E}S_{12} + L_{3E}S_{123} \\ 0 & 0 & 1 & 0 \\ 0 & 0 & 0 & 1 \end{bmatrix} \tag{1} $$

where
$C_{123} = \cos(\theta_1 + \theta_2 + \theta_3)$
$S_{123} = \sin(\theta_1 + \theta_2 + \theta_3)$

Given the joint angles as input, (1) gives a kinematic transformation from the tool to the base of the device. The Inverse Kinematic (IK) model, on the other hand, providing the joint angles in correspondence with the given position and orientation of the end-effector, has been derived mainly using geometric approach. Fig. 2a shows the simplified kinematic representation of the three link planar robotic finger. Let x, y and Φ respectively denote the given desired position and orientation of the attachment point trajectory shown in Fig. 1b. Let O_E (Fig. 2b) denotes a point (wrist center) on the robot whose position (x_e,y_e) is determined by the first $3 - h$ joints of the robot (h being the measure of number of DOF to orient the manipulator). In this case, $h = 1$ since the mechanism is planar. The coordinates of O_E are thus given by

$$ x_e = x - L_{3E}\cos\Phi \tag{2} $$

$$ y_e = y - L_{3E}\sin\Phi \tag{3} $$

Given x, y and Φ of the robot's end-effector, (2) and (3) reduce the task to compute the closed-form solution for the joint variable ensuring the corresponding (x_e,y_e). Considering the first two links and drawing projections of the robot onto a plane ⊥ to the joint axis (Fig. 2c), the unknown joint angles $(\theta_1,\theta_2,\theta_3)$ can be computed based on trigonometry as follows:

Using Law of Cosines,

$$ \cos\theta_2 = \frac{l - L_{1E}^2 - L_{2E}^2}{2L_{1E}L_{2E}} $$

Thus

$$ \theta_2 = \tan^{-1}\frac{\pm\sqrt{1-\cos^2\theta_2}}{\cos\theta_2} \tag{4} $$

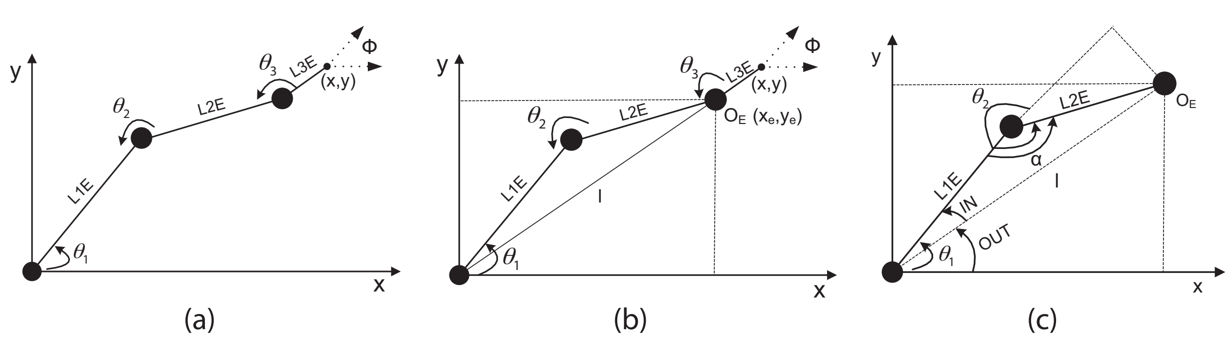

Fig. 2 – Kinematic model of the exoskeleton finger: (a) kinematic representation showing position and orientation of the end-effector, (b) description to compute O_E coordinates and (c) description to compute joint angles.

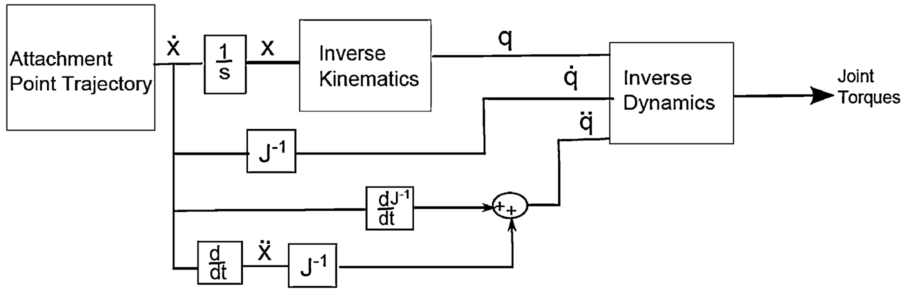

Fig. 3 – IK and dynamic model: overall block diagram.

θ_1 can be computed as

$$\theta_1 = \text{IN} + \text{OUT} = \tan^{-1}\left(\frac{L_{2E}\sin\theta_2}{L_{1E} + L_{2E}\cos\theta_2}\right) + \tan^{-1}\left(\frac{y_e}{x_e}\right) \tag{5}$$

Finally, θ_3 can be determined based on the given orientation (Φ),

$$\theta_3 = \Phi - (\theta_1 + \theta_2) \tag{6}$$

Eqs. (4)–(6) give the IK model of the proposed robotic exoskeleton.

3.2. Dynamic model

Considering the attachment point trajectory (Fig. 1b), the angular position, velocity and acceleration (denoted by q, $\dot{q}$ and $\ddot{q}$ respectively) for each finger joint of the proposed system can be computed using the derived IK model and Jacobian (7) inverse as depicted in Fig. 3.

$$J = \begin{bmatrix} a_{11} & a_{12} & a_{13} \\ a_{21} & a_{22} & a_{23} \\ 1 & 1 & 1 \end{bmatrix} \tag{7}$$

where the values of Jacobian coefficients (derived in Appendix B) are

$$a_{11} = -L_{1E}\sin\theta_1 - L_{2E}\sin(\theta_1+\theta_2) - L_{3E}\sin(\theta_1+\theta_2+\theta_3)$$
$$a_{12} = -L_{2E}\sin(\theta_1+\theta_2) - L_{3E}\sin(\theta_1+\theta_2+\theta_3)$$
$$a_{13} = -L_{3E}\sin(\theta_1+\theta_2+\theta_3)$$
$$a_{21} = L_{1E}\cos\theta_1 + L_{2E}\cos(\theta_1+\theta_2) + L_{3E}\cos(\theta_1+\theta_2+\theta_3)$$
$$a_{22} = L_{2E}\cos(\theta_1+\theta_2) + L_{3E}\cos(\theta_1+\theta_2+\theta_3)$$
$$a_{23} = L_{3E}\cos(\theta_1+\theta_2+\theta_3)$$

Using Lagrange formulation, joint-space dynamics [34] giving torque of each joint is then

$$M(q)\ddot{q} + C(q,\dot{q})\dot{q} + G(q) - J^T F = \tau$$

where $M(q)$ is the joint space inertia matrix (Table 3), $C(q,\dot{q})$ is the Coriolis matrix, $G(q)$ is the gravity vector, J is the Jacobian, F is the force exerted by the robot on a finger and τ is the joint torque.

The simulated joint torques needed to execute the desired trajectory (Fig. 1b) is shown in Fig. 4. The dashed line represents the joint torque of the base joint (active) of the proposed rehabilitation system while solid and dotted lines represent the torques corresponding to proximal and distal joints (passive) respectively. These torque values together with the system design requirements (Section 4) guided the actuators selection and design of the proposed rehabilitation system.

Table 3 – Moment of inertia of the robot's links.

Link	Mass (kg)	Length (m)	Inertia moment (kg m^2)
L_{1E}	0.12	0.08	$\begin{pmatrix} 7.35\times10^{-7} & 0 & 0 \\ 0 & 6\times10^{-5} & 0 \\ 0 & 0 & 6\times10^{-5} \end{pmatrix}$
L_{2E}	0.095	0.05	$\begin{pmatrix} 5.8\times10^{-7} & 0 & 0 \\ 0 & 2\times10^{-5} & 0 \\ 0 & 0 & 2\times10^{-5} \end{pmatrix}$
L_{3E}	0.080	0.01	$\begin{pmatrix} 4.9\times10^{-7} & 0 & 0 \\ 0 & 4\times10^{-6} & 0 \\ 0 & 0 & 4\times10^{-6} \end{pmatrix}$

4. Design requirements and optimization

The fundamental specifications for a hand exoskeleton rehabilitation system essentially include comfortability, safety, less complexity and its ability to exert perpendicular forces on the finger phalanges. The numerical design requirements can be desired ROM and ability of a device to exert force level comparable to that of the human hand. The intention to learn from nature while designing the rehabilitation device has motivated us to carry a number of experiments on the human

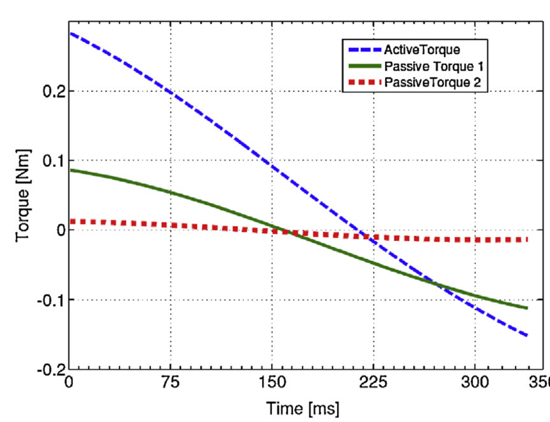

Fig. 4 – Joint torques in correspondence with the desired trajectory.

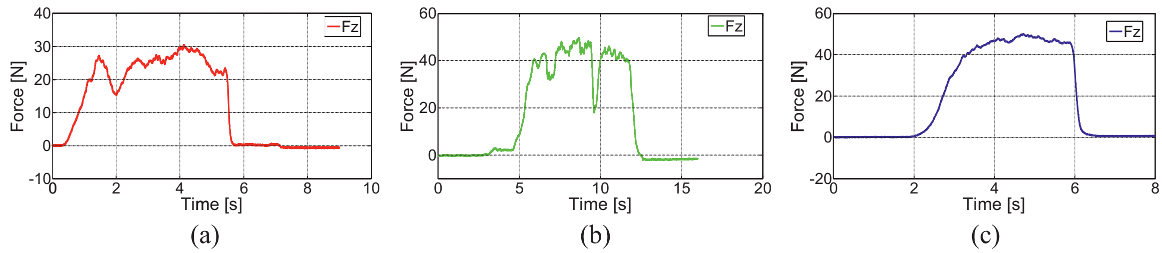

Fig. 5 – Maximum force levels exerted by index finger of (a) small, (b) medium and (c) big hand size.

hand using various sensors including data glove, load cell and force sensors. The objective was to measure capabilities and strengths of a human hand in terms of its ROM, maximum and average force levels. These results have been then mapped to the device mechanical design. Fig. 5 illustrates one such result where the maximum force levels exerted by an index finger of human hand are shown. Detailed design requirements and results of the conducted experiments are presented in [32,35].

The link lengths of the proposed rehabilitation device have been selected as a result of multi-objective optimization criteria. The optimization is based on trivial factors like kinematic mapping and collision avoidance as well as advanced workspace optimization concepts like Global Isotropy Index [36] and the requirement of exertion of perpendicular forces. Based on these, an Overall Impact Factor (OIF) has been calculated. Fig. 6 presents the result of optimization procedure [37,38] showing OIF as a function of exoskeleton link lengths $\{L_{1E}, L_{2E}\}$. The result indicates that OIF is maximized for a set of link lengths {8 cm, 5 cm} respectively. The distal exoskeleton segment (L_{3E}), which is meant to connect the human finger and the device end-effector, has been chosen as minimum (1 cm) as dictated by the mechanical integration.

5. System control

The control scheme of the proposed hand exoskeleton is based on natural human control strategies. The motivation to create human-like motions in the rehabilitation device is the driving factor to study these strategies, which reveal that the primary objective of motor coordination in the hand is to produce the smoothest possible trajectories. For safe interaction of a human hand with a rehabilitation system, essentially smooth trajectories are required. Such trajectories can be expressed in terms of a jerk function for quantification. The jerk being the derivative of acceleration w.r.t. time is mathematically equivalent to $\dddot{x}(t) = d^3x(t)/dt^3$ where $x(t)$ denotes the position of a system as a function of time. To move the human hand smoothly from one point to the other, the sum of the squared jerk along the trajectory should be minimized [39]. Thus the smoothness can be measured by the Jerk Cost Function (JCF) given by (8)

$$\mathrm{JCF} = \int_{t_1}^{t_2} \dddot{x}_1(t)^2 dt \tag{8}$$

where $x_1(t)$ is a particular trajectory starting at time t_1 and ending at time t_2. The function that most smoothly connects a starting point to a target in a given amount of time has the minimum value of the JCF. Thus by minimizing the area under this curve, a human-like trajectory has been obtained for the proposed exoskeleton device.

To execute the control strategy, a distributed control system (Fig. 7) working in a client-server mode has been implemented. The on-board controller functions as a 'server' while a dedicated laptop serves the role of a 'client'. The realized control system offers the execution of high as well as low level commands. The controller is based on a Freescale DSP (56F807) and is made up of two components (logic and power). The Controller Area Network (CAN) bus is employed to interface the controller with the application running on the laptop.

The closed-loop position control (Fig. 8) is based on the minimum jerk trajectory generation. Based on desired reference position and position sensed by the motor encoders, the control logic generates Proportional (*P*), Integrator (*I*) and Differentiator (*D*) gain coefficients. After limiting the overall coefficients, the power driver drives the motors of the device. The encoder data is sent as a feedback to close the control loop.

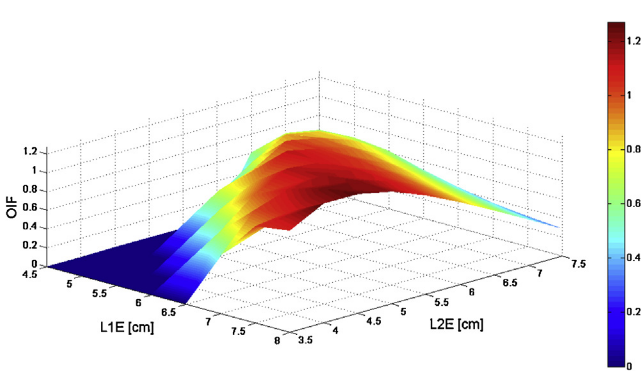

Fig. 6 – Overall Impact Factor as a function of exoskeleton link lengths.

6. System prototype and results

Using the results obtained both from the optimization procedure and human hand maximum force level measurement experiments, the first prototype of the rehabilitation system has been developed. The prototype consists of a linkage mechanism each for thumb and index finger. The

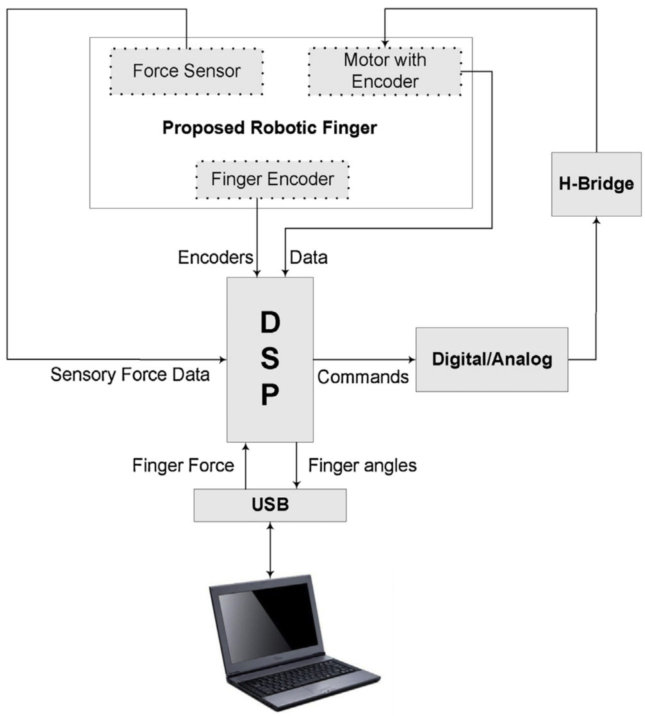

Fig. 7 – Distributed control system.

rehabilitation scheme of the remaining three fingers is same as that of index finger owing to their similarly. Each finger of the device is actuated with a separate DC brush motor (Maxon RE 25). Use of low reduction gearbox for the motor permits back-drivability of each exoskeleton finger. The device provides active DOF for flexion/extension motion while rotation of the motors on ball bearings around the vertical axis permits passive DOF for abduction/adduction motion. The CAD model of the proposed exoskeleton system is illustrated in Fig. 9.

Most of the custom designed parts have been fabricated using light aluminum while miniature components (e.g. lockers, pins) are made up of steel. The base of the robot is made up of ABS-plastic for weight reduction. The fabricated prototype of the two-fingered robotic system is shown in Fig. 10 while Table 4 summarizes key specifications of the system.

A key feature of the presented rehabilitation device concerns the design and control of the direct-driven mechanism. For guidance during rehabilitation or training, the control should have the capability to follow the desired movements or trajectories as dictated by physiotherapists. The device has been subjected to various reference inputs including step, ramp, sinusoidal etc. to investigate the dynamic characteristics of the system and to analyze the control scheme. The capability of control to track these inputs has been observed. Two cases have been considered: (i) Free motion (ii) constrained motion. In the first case, the device moves without encountering any object while in constrained case, a rubber glove packed with sponge has been used to test the device. For each reference input, five sets of readings of the motor encoder data have been recorded. For step input, the duration of the experiment was 3 s. The time course of the active joint angle of the rehabilitation device and the reference input is illustrated in Fig. 11(a) for the free motion case. The joint angle converges to its reference signal (dotted line). The deviation is very small depicting that the joint motion is reproducible. The rise time observed from the averaged data is 0.22 s. For constrained case, step response of the device is shown in Fig. 11(b). In terms of physical values, this plot resembles significantly with the response illustrated in Fig. 11 (a) implying high reproducibility. The joint angles can closely track the desired signal. The rise time in this case is 0.33 s. This value is different from the rise time in the first case due to the rubber elasticity.

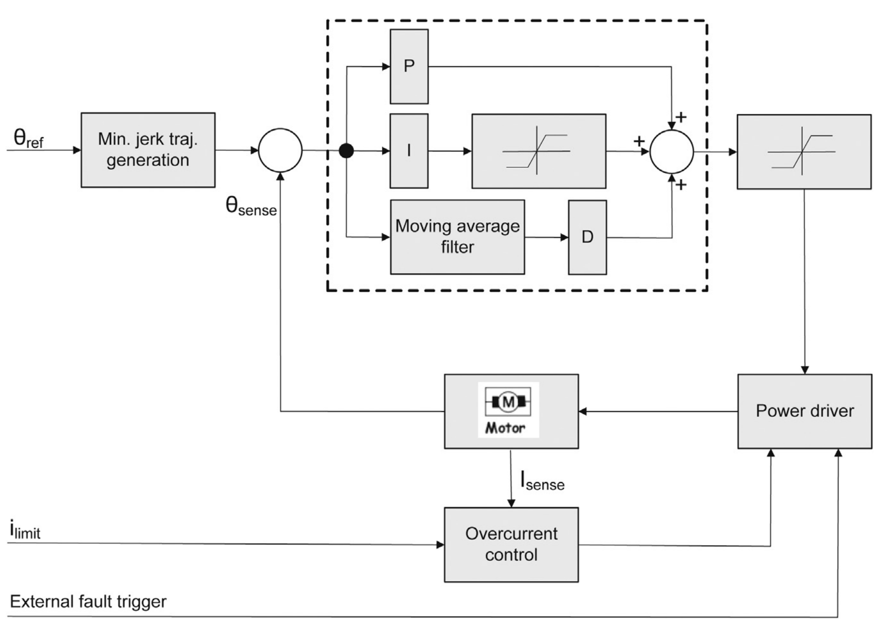

Fig. 8 – Control architecture of the proposed robotic system.

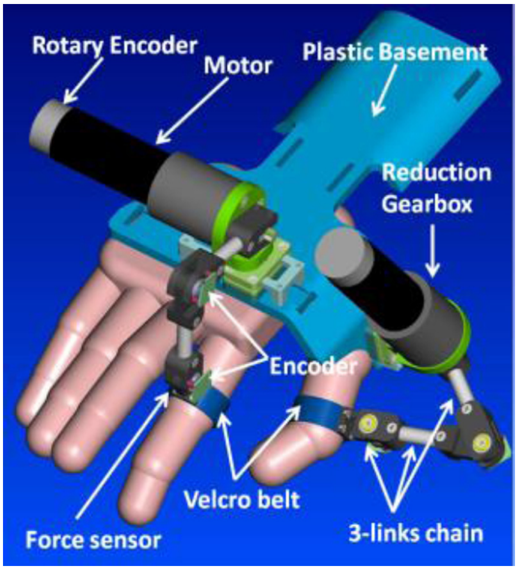

Fig. 9 – 3D CAD model of the proposed rehabilitation device.

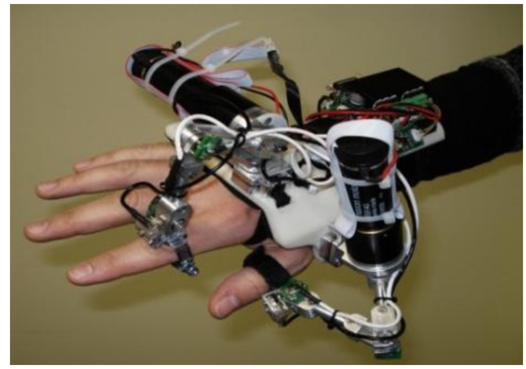

Fig. 10 – Fabricated prototype of the proposed robotic system.

Table 4 – Specifications of the proposed system.

Specification	Value
Degrees of Freedom/finger	4 (1 active)
Maximum continuous force	45 N
Actuator torque capability (stall torque)	3.6 N m
Weight of the device excluding actuators	0.4 kg
Total weight of the device	1 kg
Force sensor resolution	0.01 N
Position sensor resolution	0.0879°

Exercises using a rehabilitation device essentially include execution of finger flexion-extension cycles. This, in terms of control, means tracking a sinusoidal trajectory. Fig. 12(a) and (b) shows the sinusoidal response of the proposed device in case of free movement and constrained motion respectively. As illustrated, the joint angles can continuously track the time-varying reference input in their close proximity.

Another experiment addressed the control performance in case of a user wearing the exoskeleton device. In this self-motion control case, the objective was to evaluate the ability of the system in sustaining a constraint. The user varied the applied force while the controller has been set to ensure a constant position. In view of the fact that the proposed rehabilitation device can provide bidirectional forces, a bidirectional constraint was applied. Fig. 13 illustrates the position control response of the system.

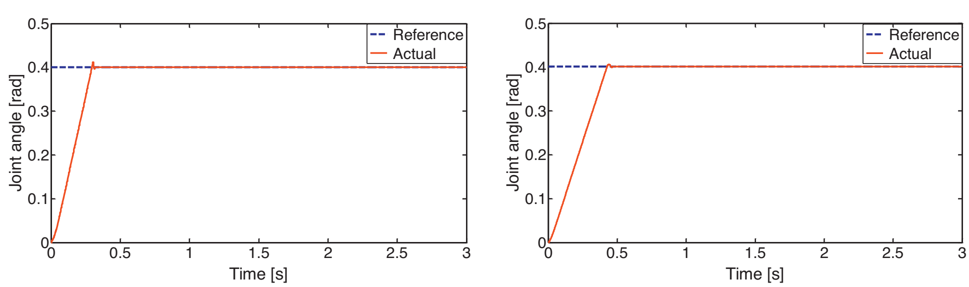

Fig. 11 – Device step response in case of (a) free motion and (b) constrained motion.

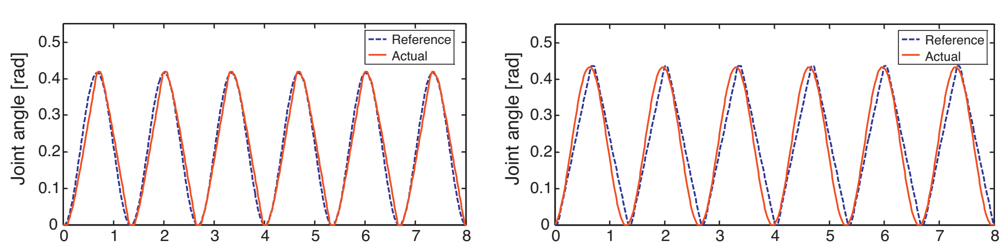

Fig. 12 – Device sinusoidal response in case of (a) free motion and (b) constrained motion.

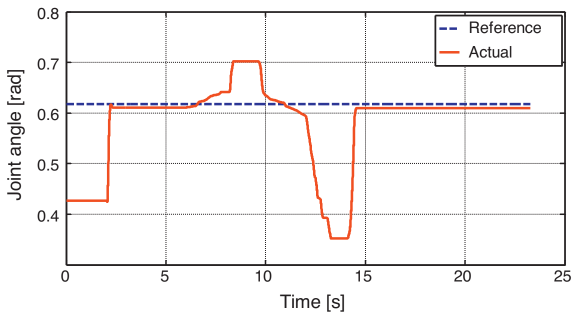

Fig. 13 – Constraint stabilization response.

7. Conclusion

This paper presents a novel hand exoskeleton based rehabilitation device that is aimed at patients' recovery during post-stroke activities by practicing fingers flexion and extension. Based on the proposed direct-driven under-actuated mechanism, the device design has been supported by optimization results, derivation of design requirements, modeling and control algorithm. Such a mechanism based on the direct transmission of force/torque offers several advantages over tendon-driven systems. The mechanism does not require continuous control of cable tensioning and avoids issues arising because of intrinsic friction. The direct driven devices also exhibit other benefits in terms of wide stiffness range and enhanced force bandwidth as compared with cable based systems because the later act as a stiff spring thus limiting end-effector stiffness. Other features that make the present work distinguishing among existing systems include human hand compatibility, portability, less complexity and easy removal/donning. The proposed rehabilitation device provides adequate force levels for executing ADL. Trying to match the human hand capabilities resulted in a device with natural ROM and force levels (of 45 N) beyond any existing system's capability. Being a portable system, the presented device has a great potential in prosthetics as well as for assistance. The comfort, because of ease in fitting adjustment and removal, permits the extended use of the system without causing fatigue to the wearer even after long periods (e.g. 1–2 h of operation).

The pilot study based on series of experiments indicates that the device has the capability to move the finger digits and to track various trajectories. Nearly every possible motion trajectory can be followed with adequate accuracy. The device provides position feedback as well as offers monitoring of forces exerted by the wearer during rehabilitation. These feedbacks are quantitative indicators of recovery and can facilitate physical therapy plans. More clinical trials are intended to further access the device performance. With the help of rehabilitation professionals, we are currently developing rehabilitation strategies to test the exoskeleton on patients after meeting medical safety standards. The proposed device is anticipated to have a great potential in rehabilitation of the impaired hand.

In addition to rehabilitation, the proposed exoskeleton, owing to its portability, can also find application as an assistive device. Translating the requirement of maximum force strength of a human hand in the device design by appropriate actuator selection resulted in a system exhibiting higher force levels (45 N) beyond any existing rehabilitation device. However, in our daily life, it is quite seldom that we need such huge force levels. To enhance the portability of the exoskeleton, it is simple to substitute the current actuators with smaller ones for reducing weight and size while still providing enough force levels for many of the daily life applications. Future work includes developing strategies to control the exoskeleton through brain signals and to finally integrate the device in a wheelchair based robot for outdoor use [40].

Financial support

Italian Institute of Technology (IIT), University of Genova provided funding and required resources to conduct this research, while COMSATS, Islamabad, Pakistan provided support for preparation of this article.

Acknowledgement

The authors would like to extend their thanks to Dr. Emanuele and therapists at Ospedale San Martino, Genoa for their valuable comments and suggestions. Thanks to University of Genova for providing funding and required resources for this research. Special regards to Dr. Muhammad Fasih Uddin Butt, Director of Modeling and Simulation Lab. at CIIT, Islamabad, Pakistan to provide resources and environment to facilitate the write-up of this manuscript.

Appendix A. Derivation of overall transformation matrix

Based on the determined DH parameters (Table 2) and using the general form of Transformation matrix i.e.

$$ {}^{i-1}_{\ \ i}T = \begin{bmatrix} C\theta_i & -S\theta_i & 0 & a_{i-1} \\ S\theta_i C\alpha_{i-1} & C\theta_i C\alpha_{i-1} & -S\alpha_{i-1} & -d_i S\alpha_{i-1} \\ S\theta_i S\alpha_{i-1} & C\theta_i S\alpha_{i-1} & C\alpha_{i-1} & d_i C\alpha_{i-1} \\ 0 & 0 & 0 & 1 \end{bmatrix} $$

the link transformation matrices from each link of the robot in its neighboring link can be written as

$$ {}^{0}_{1}T = \begin{bmatrix} C_1 & -S_1 & 0 & 0 \\ S_1 & C_1 & 0 & 0 \\ 0 & 0 & 1 & 0 \\ 0 & 0 & 0 & 1 \end{bmatrix} $$

$$ {}^{1}_{2}T = \begin{bmatrix} C_2 & -S_2 & 0 & L_{1E} \\ S_2 & C_2 & 0 & 0 \\ 0 & 0 & 1 & 0 \\ 0 & 0 & 0 & 1 \end{bmatrix} $$

$$ {}^{2}_{3}T = \begin{bmatrix} C_3 & -S_3 & 0 & L_{2E} \\ S_3 & C_3 & 0 & 0 \\ 0 & 0 & 1 & 0 \\ 0 & 0 & 0 & 1 \end{bmatrix} $$

$$ {}^{3}_{4}T = \begin{bmatrix} 1 & 0 & 0 & L_{3E} \\ 1 & 1 & 0 & 0 \\ 0 & 0 & 1 & 0 \\ 0 & 0 & 0 & 1 \end{bmatrix} $$

The compound transformation from end-effector (frame {4}) to base (frame {0}) yields

$$ {}^{0}_{4}T = {}^{0}_{1}T \quad {}^{1}_{2}T \quad {}^{2}_{3}T \quad {}^{3}_{4}T $$
$$ = \begin{bmatrix} C_{123} & -S_{123} & 0 & L_{1E}C_1 + L_{2E}C_{12} + L_{3E}C_{123} \\ S_{123} & C_{123} & 0 & L_{1E}S_1 + L_{2E}S_{12} + L_{3E}S_{123} \\ 0 & 0 & 1 & 0 \\ 0 & 0 & 0 & 1 \end{bmatrix} $$

where the Rotation matrix is given by

$$ {}^{0}_{4}R = \begin{bmatrix} C_{123} & -S_{123} & 0 \\ S_{123} & C_{123} & 0 \\ 0 & 0 & 1 \end{bmatrix} $$

Appendix B. Derivation of Jacobian matrix

Considering a Revolute joint, the general form of angular and linear velocities of a link can be written as

$$ {}^{i+1}\omega_{i+1} = {}^{i+1}_{i}R\,{}^{i}\omega_i + \dot{\theta}_{i+1}\,{}^{i+1}\hat{z}_{i+1} $$
$$ {}^{i+1}v_{i+1} = {}^{i+1}_{i}R({}^{i}v_i + {}^{i}\omega_i \, X \, {}^{i}P_{i+1}) $$

In case of the proposed robotic system, for $i = 0$,

$$ {}^{1}\omega_1 = \begin{bmatrix} 0 \\ 0 \\ \dot{\theta}_1 \end{bmatrix} \qquad {}^{1}v_1 = \begin{bmatrix} 0 \\ 0 \\ 0 \end{bmatrix} $$

For $i = 1$,

$$ {}^{2}\omega_2 = \begin{bmatrix} 0 \\ 0 \\ \dot{\theta}_1 + \dot{\theta}_2 \end{bmatrix} \qquad {}^{2}v_2 = \begin{bmatrix} L_{1E}S_2\dot{\theta}_1 \\ L_{1E}C_2\dot{\theta}_1 \\ 0 \end{bmatrix} $$

For $i = 2$,

$$ {}^{3}\omega_3 = \begin{bmatrix} 0 \\ 0 \\ \dot{\theta}_1 + \dot{\theta}_2 + \dot{\theta}_3 \end{bmatrix} \qquad {}^{3}v_3 = \begin{bmatrix} L_{1E}S_{23}\dot{\theta}_1 + L_{2E}S_3(\dot{\theta}_1 + \dot{\theta}_2) \\ L_{1E}C_{23}\dot{\theta}_1 + L_{2E}C_3(\dot{\theta}_1 + \dot{\theta}_2) \\ 0 \end{bmatrix} $$

For $i = 3$,

$$ {}^{4}\omega_4 = {}^{3}\omega_3 = \begin{bmatrix} 0 \\ 0 \\ \dot{\theta}_1 + \dot{\theta}_2 + \dot{\theta}_3 \end{bmatrix} $$

$$ {}^{4}v_4 = \begin{bmatrix} L_{1E}S_{23}\dot{\theta}_1 + L_{2E}S_3(\dot{\theta}_1 + \dot{\theta}_2) \\ L_{1E}C_{23}\dot{\theta}_1 + L_{2E}C_3(\dot{\theta}_1 + \dot{\theta}_2) + L_{3E}(\dot{\theta}_1 + \dot{\theta}_2 + \dot{\theta}_3) \\ 0 \end{bmatrix} $$

Rewriting ${}^{4}v_4$ expression in matrix form,

$$ {}^{4}v_4 = \begin{bmatrix} L_{1E}S_{23} + L_{2E}S_3 & L_{2E}S_3 & 0 \\ L_{1E}C_{23} + L_{2E}C_3 + L_{3E} & L_{2E}C_3 + L_{3E} & L_{3E} \\ 0 & 0 & 0 \end{bmatrix} \begin{bmatrix} \dot{\theta}_1 \\ \dot{\theta}_2 \\ \dot{\theta}_3 \end{bmatrix} $$

Transforming w.r.t. Base frame {0},

$$ {}^{0}v_4 = {}^{0}_{4}R\,{}^{4}v_4 = \begin{bmatrix} C_{123} & -S_{123} & 0 \\ S_{123} & C_{123} & 0 \\ 0 & 0 & 0 \end{bmatrix} $$
$$ \times \begin{bmatrix} L_{1E}S_{23} + L_{2E}S_3 & L_{2E}S_3 & 0 \\ L_{1E}C_{23} + L_{2E}C_3 + L_{3E} & L_{2E}C_3 + L_{3E} & L_{3E} \\ 0 & 0 & 0 \end{bmatrix} \begin{bmatrix} \dot{\theta}_1 \\ \dot{\theta}_2 \\ \dot{\theta}_3 \end{bmatrix} $$
$$ = \begin{bmatrix} a_{11} & a_{12} & a_{13} \\ a_{21} & a_{22} & a_{23} \\ 0 & 0 & 0 \end{bmatrix} \begin{bmatrix} \dot{\theta}_1 \\ \dot{\theta}_2 \\ \dot{\theta}_3 \end{bmatrix} \tag{B1} $$

where

$a_{11} = -L_{1E}\sin\theta_1 - L_{2E}\sin(\theta_1 + \theta_2) - L_{3E}\sin(\theta_1 + \theta_2 + \theta_3)$
$a_{12} = -L_{2E}\sin(\theta_1 + \theta_2) - L_{3E}\sin(\theta_1 + \theta_2 + \theta_3)$
$a_{13} = -L_{3E}\sin(\theta_1 + \theta_2 + \theta_3)$
$a_{21} = L_{1E}\cos\theta_1 + L_{2E}\cos(\theta_1 + \theta_2) + L_{3E}\cos(\theta_1 + \theta_2 + \theta_3)$
$a_{22} = L_{2E}\cos(\theta_1 + \theta_2) + L_{3E}\cos(\theta_1 + \theta_2 + \theta_3)$
$a_{23} = L_{3E}\cos(\theta_1 + \theta_2 + \theta_3)$

Similarly, rewriting ${}^{4}\omega_4$ expression in matrix form,

$$ {}^{4}\omega_4 = \begin{bmatrix} 0 & 0 & 0 \\ 0 & 0 & 0 \\ 1 & 1 & 1 \end{bmatrix} \begin{bmatrix} \dot{\theta}_1 \\ \dot{\theta}_2 \\ \dot{\theta}_3 \end{bmatrix} $$

Transforming w.r.t. Base frame {0},

$$ {}^{0}\omega_4 = {}^{0}_{4}R\,{}^{4}\omega_4 = \begin{bmatrix} C_{123} & -S_{123} & 0 \\ S_{123} & C_{123} & 0 \\ 0 & 0 & 1 \end{bmatrix} \begin{bmatrix} 0 & 0 & 0 \\ 0 & 0 & 0 \\ 1 & 1 & 1 \end{bmatrix} \begin{bmatrix} \dot{\theta}_1 \\ \dot{\theta}_2 \\ \dot{\theta}_3 \end{bmatrix} $$
$$ = \begin{bmatrix} 0 & 0 & 0 \\ 0 & 0 & 0 \\ 1 & 1 & 1 \end{bmatrix} \begin{bmatrix} \dot{\theta}_1 \\ \dot{\theta}_2 \\ \dot{\theta}_3 \end{bmatrix} \tag{B2} $$

Combining linear velocities given by (B1) and angular velocity (B2),

$$ \begin{bmatrix} v_x \\ v_y \\ \omega_z \end{bmatrix} = \begin{bmatrix} a_{11} & a_{12} & a_{13} \\ a_{21} & a_{22} & a_{23} \\ 1 & 1 & 1 \end{bmatrix} \begin{bmatrix} \dot{\theta}_1 \\ \dot{\theta}_2 \\ \dot{\theta}_3 \end{bmatrix} = J \begin{bmatrix} \dot{\theta}_1 \\ \dot{\theta}_2 \\ \dot{\theta}_3 \end{bmatrix} $$

where J is the Jacobian matrix whose coefficients are given by (B1).

REFERENCES

[1] Ferris DP. The exoskeletons are here. J Neuroeng Rehabil 2009;6:17.

[2] Rathore SS, Hinn AR, Cooper LS, Tyroler HA, Posamond WD. Characterization of incident stroke signs and symptoms: findings from the atherosclerosis risk in communities study. Stroke 2002;33(11):2718–21.

[3] Duncan PW, Bode RK, Min Lai S, Perera S. Rasch analysis of a new stroke specific outcome scale: the stroke impact scale. Arch Phys Med Rehabil 2003;84(7):950–63.

[4] Lambercy O, Dovat L, Gassert R, Burdet E, Teo CL, Milner T. A haptic knob for rehabilitation of hand function. IEEE Trans Neural Syst Rehabil Eng 2007;15(3): 356–66.

[5] Kwakkel G, Kollen BJ, van der Grond J, Prevo AJ. Probability of regaining dexterity in the flaccid upper limb: impact of

severity of paresis and time since onset in acute stroke. Stroke 2003;34(9):2181–6.
[6] Kamper DG, Harvey RL, Suresh S, Rymer WZ. Relative contributions of neural mechanisms versus muscle mechanics in promoting finger extension deficits following stroke. Muscle Nerve 2003;28(3):309–18.
[7] Carey JR, Durfee WK, Bhatt E, Nagpal A, Weinstein SA, Anderson KM, et al. Comparison of finger tracking versus simple movement training via telerehabilitation to alter hand function and cortical reorganization after stroke. Neurorehabil Neural Repair 2007;21(3):216–32.
[8] Fischer HC, Stubblefield K, Kline T, Luo X, Kenyon RV, Kamper DG. Hand rehabilitation following stroke: a pilot study of assisted finger extension training in a virtual environment. Top Stroke Rehabil 2007;14(1):1–12.
[9] JACE H440 hand CPM. http://www.jacesystems.com/products/hand_h440.htm [accessed 24.05.13].
[10] Fu Y, Wang P, Wang S. Development of a multi-DOF exoskeleton based machine for injured fingers. Proc IEEE/RSJ International Conference on Intelligent RObots and Systems (IROS), Nice. 2008. pp. 1946–51.
[11] Brokaw EB, Black I, Holley RJ, Lum PS. Hand Spring Operated Movement Enhancer (HandSOME): a portable, passive hand exoskeleton for stroke rehabilitation. IEEE Trans Neural Syst Rehabil Eng 2011;19(4):391–9.
[12] Tzafestas CS. Whole-hand kinesthetic feedback and haptic perception in dextrous virtual manipulation. IEEE Trans Syst Man Cybern B: Cybern 2003;33(1):100–13.
[13] Stergiopoulos P, Fuchs P, Laurgeau C. Design of a 2-finger hand exoskeleton for VR grasping simulation. Proc Eurohaptics, Dublin. 2003. pp. 80–93.
[14] Richardson BL, Wuillemin DB, Symmons MA, Accardi R. The exograsp delivers tactile and kinaesthetic information about virtual objects. Proc IEEE Tencon, Melbourne. 2005. pp. 1–3.
[15] Folgheraiter M, Gini G, Vercesi DL. A glove interface with tactile feeling display for humanoid robotics and virtual reality systems. Proc International Conference on Informatics in Control, Automation and Robotics (ICINCO), Barcelona; 2005.
[16] Lelieveld MJ, Maeno T, Tomiyama T. Design and development of two concepts for a 4 DOF portable haptic interface with active and passive multi-point force feedback for the index finger. Proc ASME International Design Engineering Technical Conferences (IDETC) and Computers and Information in Engineering (CIE) Conference, Philadelphia; 2006.
[17] Iqbal J, Tsagarakis NG, Caldwell DG. Design of a wearable direct-driven optimized hand exoskeleton device. Proc 4th International Conference on Advances in Computer–Human Interactions (ACHI), Gosier; 2011. pp. 142–6.
[18] Bouzit M, Burdea G, Popescu G, Boian R. The Rutgers Master II-New Design force-feedback glove. IEEE/ASME Trans Mechatron 2002;12(4):399–407.
[19] Ito S, Kawasaki H, Ishigure Y, Natsume M, Mouri T, Nishimoto Y. A design of fine motion assist equipment for disable hand in robotic rehabilitation system. J Franklin Inst 2011;348(1):79–89.
[20] Sarakoglou I, Tsagarakis N, Caldwell D. Occupational and physical therapy using a hand exoskeleton based exerciser. Proc IEEE/RSJ International Conference on Intelligent RObots and Systems (IROS), Sendai; 2004. pp. 2973–8.
[21] Wege A, Hommel G. Development and control of a hand exoskeleton for rehabilitation of hand injuries. Proc IEEE/RSJ International Conference on Intelligent RObots and Systems (IROS), Edmonton. 2005. pp. 3046–51.
[22] Lenzi T, De Rossi S, Vitiello N, Chiri A, Roccella S, Giovacchini F, et al. The neuro-robotics paradigm: NEURARM, NEUROExos, HANDEXOS. Proc 31st Annual International Conference of the IEEE Engineering in Medicine and Biology Society (EMBS), Minneapolis. 2009. pp. 2430–3.
[23] Schabowsky CN, Godfrey SB, Holley RJ, Lum PS. Development and pilot testing of HEXORR: Hand EXOskeleton Rehabilitation Robot. J Neuroeng Rehabil 2010;7:36.
[24] Wang J, Li J, Zhang Y, Wang S. Design of an exoskeleton for index finger rehabilitation. Proc 31st Annual International Conference of the IEEE Engineering in Medicine and Biology Society (EMBS), Minneapolis. 2009. pp. 5957–60.
[25] Merians AS, Jack D, Boian R, Tremaine M, Burdea GC, Adamovich SV, et al. Virtual reality-augmented rehabilitation for patients following stroke. Phys Ther 2002;82(9):898–915.
[26] Dovat L, Lambercy O, Salman B, Johnson V, Milner T, Gassert R, et al. A technique to train finger coordination and independence after stroke. Disabil Rehabil Assist Technol 2010;5(4):279–87.
[27] Amadeo – for all phases of neurological rehabilitation. http://tyromotion.com/en/products/amadeo/overview [accessed 24.05.13].
[28] Frisoli A, Simoncini F, Bergamasco M. Mechanical design of a haptic interface for the hand. Proc ASME Design Engineering Technical Conferences, Montreal; 2002. pp. 25–32.
[29] Tsagarakis N, Caldwell D. Development and control of a 'Soft-actuated' exoskeleton for use in physiotherapy and training. Auton Robots Spec Issue Rehabil Robot 2003;15:21–33.
[30] Ochoa J, Dev Narasimhan YJ, Kamper DG. Development of a portable actuated orthotic glove to facilitate gross extension of the digits for therapeutic training after stroke. Proc 31st Annual International Conference of the IEEE Engineering in Medicine and Biology Society (EMBS), Minneapolis. 2009. pp. 6918–21.
[31] Manzoor S, Islam RU, Khalid A, Samad A, Iqbal J. An open-source multi-DOF articulated robotic educational platform for autonomous object manipulation. Robot Comput Integr Manuf 2014;30(3):351–62.
[32] Iqbal J, Tsagarakis N, Fiorilla AE, Caldwell DG. Design requirements of a hand exoskeleton robotic device. Proc 14th IASTED International Conference on Robotics and Applications (RA), Cambridge, MA. 2009. pp. 44–51.
[33] Spong MW, Vidyasagar M. Robot dynamics and control. New Jersey, United States: John Wiley and Sons; 1989.
[34] Awrejcewicz J. Classical mechanics. Kinematics and statics. New York: Springer; 2012.
[35] Iqbal J, Tsagarakis NG, Caldwell DG. A human hand compatible optimised exoskeleton system. Proc IEEE International Conference on RObotics and BIOmimetics (ROBIO), Tianjin; 2010. pp. 685–90.
[36] Stocco L, Salcudean SE, Sassani F. Fast constrained global minimax optimization of robot parameters. Robotica 1998;16(6):595–605.
[37] Iqbal J, Tsagarakis N, Caldwell D. Design optimization of a hand exoskeleton rehabilitation device. Proc Robotics Sciences and Systems (RSS), Workshop on Understanding the Human Hand for Advancing Robotic Manipulation Proceedings, Seattle; 2009. p. 44–5.
[38] Iqbal J, Tsagarakis N, Fiorilla AE, Caldwell D. A portable rehabilitation device for the hand. Proc 32nd IEEE Annual International Conference of Engineering in Medicine and Biology Society (EMBS), Buenos Aires; 2010. pp. 3694–7.
[39] Shadmehr R, Wise SP. Supplementary documents for computational neurobiology of reaching and pointing. Cambridge, MA: MIT Press; 2005.
[40] Khan AA, Riaz S, Iqbal J. Surface estimation of a pedestrian walk for outdoor use of power wheelchair based robot. Life Sci J 1097-81352013;10(3):1697–704.